# Supramolecular architecture elucidation of the room temperature columnar mesophases exhibited by mixed-valent diruthenium alkoxybenzoates†

**Zulema D. Chaia,‡[a] Marcia C. Rusjan,§[a] Maria Ana Castro,[a] Bertrand Donnio,[b] Benoit Heinrich,[b] Daniel Guillon,[b] Ricardo F. Baggio[d] and Fabio D. Cukiernik*[ac]**

***Received 15th January 2009, Accepted 6th April 2009***
***First published as an Advance Article on the web 8th June 2009***
**DOI: 10.1039/b900779b**

Three series of mesogenic coordination polymers based on mixed-valent diruthenium tetracarboxylates, namely $Ru_2$(3,4-B2OC*n*)$_4$Cl, $Ru_2$(3,5-B2OC*n*)$_4$Cl and $Ru_2$(3,4,5-B3OC*n*)$_4$Cl [3,4-B2OC*n* = 3,4-$(C_nH_{2n+1}O)_2C_6H_3CO_2^-$, 3,5-B2OC*n* = 3,5-$(C_nH_{2n+1}O)_2C_6H_3CO_2^-$ and 3,4,5-B3OC*n* = 3,4,5-$(C_nH_{2n+1}O)_3C_6H_2CO_2^-$] have been synthesized and characterized, with the aim of obtaining columnar liquid crystalline phases. These equatorial B*m*OC*n* ligands have been selected under the assumption that they will efficiently fill the intermolecular space around the axial Cl atoms, thus warranting a parallel arrangement of the polymeric $\cdots Ru_2$–Cl–$Ru_2$–Cl$\cdots$ strands in the crystalline phase, which should facilitate the occurrence of Col mesophases. The liquid crystalline character of the synthesized compounds has been studied by means of polarized optical microscopy, differential scanning calorimetry, and variable temperature X-ray diffraction. They all exhibit thermotropic $Col_H$ mesophases, the 3,4-B2OC*n* derivatives also exhibit a lamellar mesophase. Many of the studied compounds exhibit room temperature mesomorphism. The thermal stability domain of the $Col_H$ mesophases of the 3,5-B2OC*n* and 3,4,5-B3OC*n* derivatives is remarkably wide, from below 0 °C to *ca.* 300 °C in some cases. Based on pieces of structural information coming from XRD experiments, dilatometry, and local probes (magnetic susceptibility measurements, resonance Raman and IR spectroscopies, and Exafs) we suggest a model for the structural arrangement of the polymeric strands in the mesophase, in which the central polar backbone of the polymeric strands is in a *zig-zag* conformation, surrounded by a continuum of molten aliphatic chains. A crystallographic study of the non-mesogenic light homologue $Ru_2$(3,4,5-B3OC2)$_4$Cl confirms these aspects of the model, and shows the predicted preorganization of the polymeric strands in the crystalline phase.

## Introduction

Coordination polymers are a wide class of materials receiving growing attention in basic research due to two main reasons. Owing to the characteristics of the coordination bond, they provide a unique possibility of studying the strong relationship between molecular properties and supramolecular architecture in molecular materials.[1–3] Indeed, they usually consist of coordination compounds exhibiting interesting molecular properties, which act as building blocks for extended systems, linked by bridging ligands chosen in order to provide some selected properties: magnetic interactions, electron delocalization, structural organization, *etc*. This combination of molecular properties, structural organization and inter-unit interactions (a key aspect of the molecular materials paradigm),[4] can give rise to specific magnetic,[5] optical or transport (electronic, energy)[6] macroscopic properties. This makes coordination polymers attractive materials as they are potential candidates for opto-electronic and related applications, which is the second reason for the increasing number of studies. Different issues have been explored in the last two decades; among the various building blocks thoroughly examined, metallophtalocyanines have been studied as molecular wires or NLO materials,[7,8] Cu or Mn acetylacetonates or oxalate as precursors to molecular magnets,[9]

[a]*INQUIMAE, Departamento de Química Inorgánica, Analítica y Química Física, Facultad de Ciencias Exactas y Naturales, Universidad de Buenos Aires, Pab. II, Ciudad Universitaria, C1428EHA Buenos Aires, Argentina*
[b]*Institut de Physique et Chimie des Matériaux de Strasbourg (IPCMS), 23 rue de Loess, BP43 67034 Strasbourg Cedex 2, France*
[c]*Instituto de Ciencias, Universidad Nacional de General Sarmiento, J. M. Gutierrez 1150, B1613GSX Los Polvorines, Prov. Buenos Aires, Argentina*
[d]*Departamento de Física – Comisión Nacional de Energía Atómica, Av. Gral. Paz 1499 (1650) San Martín, Prov. Buenos Aires, Argentina. E-mail: fabioc@qi.fcen.uba.ar*

† Electronic supplementary information (ESI) available: Detailed synthesis procedures for selected compounds, IR and elemental analysis data, DSC traces, XRD patterns for selected compounds, assignment of the XRD peaks for all the studied compounds at selected temperatures, details on the treatment of the magnetic susceptibility data and the calculation of molecular volumes, complete sets of parameters corresponding to the magnetic studies, the temperature-dependent RR studies and Exafs refinement, as well as selected geometric parameters and the CIF file for $Ru_2$(3,4,5-B3OC2)$_4$Cl are available. Figures describing the possible conformers of $Ru_2$(3,4-B2OC*n*)$_4$Cl, the labeling scheme for $Ru_2$(3,4,5-B3OC2)$_4$Cl and the dilatometric study are also included. CCDC reference number 716719. For ESI and crystallographic data in CIF or other electronic format see DOI: 10.1039/b900779b

‡ Present address: Water Purification Supplies, Dervich, 3149 John P. Curce Dr. Bldg. 1A, Bay 4, Pembroke Park, FL 33009, USA.
§ Present address: Laboratorios Raffo, Agustín Alvarez 4845, B1603APO, Villa Marteli, Buenos Aires, Argentina.

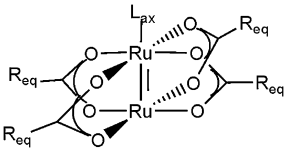


**Chart 1** General sketch for the diruthenium carboxylates ($L_{ax}$ = axial ligand; $R_{eq}$ = equatorial ligand).

prussian blue analogs have been studied as magnets, photomagnets as well as photoconductors.[10] More recently, diruthenium carboxylates (see Chart 1),[11,12] usually studied from the inorganic chemistry viewpoint, have been used as building blocks for advanced materials.[13,14]

They exhibit the lantern structure typical of different bimetallic carboxylates but show very peculiar properties which makes them very attractive candidates for fundamental studies in the materials chemistry field:[11] they can exist as stable species in two different oxidation states (II,II) and (II,III), they can polymerize if the axial positions are occupied by bridging ligands, their molecular properties and intermolecular interactions can be tuned by an appropriate choice of the equatorial carboxylates and axial ligands, they exhibit multiple metal-metal bonds, as well as paramagnetic ground states (S = 3/2 for the (II,III) species, S = 1 for the (II,II) species), undergoing large zero-field splitting, and can interact magnetically with appropriate partners.

Such compounds offer an additional advantage: most of the long-chain derivatives exhibit liquid crystalline phases, mainly of the columnar type,[11,13,15] from which they might, in principle, easily be processed in order to obtain macroscopically oriented samples. Metal-containing liquid crystals (metallomesogens)[16–18] are materials which have received much attention since their beginning as a research field, 25 years ago, but which have not still showed all their potential. Several types of metallomesogens have been synthesized and their LC and other physical properties have been investigated. However, metallomesogens based on coordination polymers are not usual; examples of coordination polymers giving rise to columnar mesophases are scarce.[16,17,18g] In recent years we have been studying the molecular structure-mesomorphic properties relationship of diruthenium (II,III) tetracarboxylates and related bimetallic carboxylates, and found that a key factor for obtaining columnar mesophases with these building blocks is to fill the intermolecular space in an intracolumnar way. As a matter of fact, mixed-valent diruthenium (II,III) compounds in which the equatorial positions are occupied by linear aliphatic carboxylates and the axial position by a small anion like chloride were found to be not mesogenic, whereas compounds in which the equatorial carboxylates contain linear aliphatic chains, but the axial ligands are long-chain anions (carboxylate, dodecylsulfate, octylsulfonate) are mesogenic.[13a,b,19] The reason for such a behavior is that a parallel arrangement of the polymeric or pseudo-polymeric strands of bimetallic carboxylates in the crystalline state has been considered a prerequisite for the occurrence of thermotropic columnar mesophases.[16,20] In the case of diruthenium (II,III) derivatives containing chloride as the axial anion, the free space created by the small anion should be filled by the equatorial carboxylates in order to prevent perpendicular arrangements in which this free space is filled by aliphatic chains of a neighbouring strand, thus forcing the adoption of a perpendicular position—as found in the crystalline structures of the butanoato[21] and pentanoato[22] derivatives. The presence of an axial anion bearing a long aliphatic chain efficiently fills the intermolecular space, giving rise to parallel arrangements of the polymeric strands in the crystalline phase. However, these compounds exhibit two big disadvantages: the transition temperatures to the columnar mesophase are usually very high (140 to 190 °C), and their thermal stability is quite limited, starting to decompose in some cases even at 175 °C (just 20 °C above the melting temperature).[23] The derivatives containing chloride as the axial anion are revealed to be much more thermally stable (decomposition takes place above 300 °C, in the isotropic state).[23b] The question would be how to induce mesomorphism while keeping chloride as axial anion. We showed in preliminary works[13b,24] that the intermolecular space can also be successfully filled in an intracolumnar way by using bulky equatorial carboxylates—a similar strategy to the one used succesfully in rhodium-pyrazine coordination polymers,[25] and introduced some examples using di- or tri-alkoxy substituted benzoates in equatorial positions.

We present in this report a complete study on the mesomorphic properties of polymeric diruthenium (II,III) alkoxybenzoate chloride complexes, including three series of compounds (Chart 2): those having 3,4-di(alkoxy)benzoates as equatorial ligands [3,4-$(C_nH_{2n+1}O)_2C_6H_3CO_2^-$, abbrev: 3,4-B2OC*n*], those having 3,5-di(alkoxy)benzoates as equatorial ligands [3,5-$(C_nH_{2n+1}O)_2C_6H_3CO_2^-$, abbrev: 3,5-B2OC*n*], and those having 3,4,5-tri(alkoxy)benzoates as equatorial ligands [3,4,5-$(C_nH_{2n+1}O)_3C_6H_2CO_2^-$, abbrev: 3,4,5-B3OC*n*]. The influence of the molecular structure on the mesomorphic properties (studied by POM, DSC and XRD) is analyzed, and the conditions for room temperature mesomorphism in these systems are established. A model for the supramolecular architecture in the mesophase is proposed on the basis of structural information coming from a combination of macro-structural techniques (XRD studies, dilatometry, density measurements), micro-structural probes (SQUID, Resonance Raman, Exafs, IR), and modelling of molecular volumes. A single-crystal XRD determination of the structure of a short-chain non-mesogenic homologue confirms the main features of the proposed model.

## Experimental section

### Synthesis and characterization

The synthesis and purification of the alkoxybenzoic acids used as ligands have been described elsewhere.[25] They all showed satisfactory $^1$H-NMR and IR spectra as well as elemental analysis. All the studied compounds, namely $Ru_2$(3,4,5-B3OC*n*)$_4$Cl (for *n* = 2, 6, 8, 10, 12, 14, 16 and 18), $Ru_2$(3,4-B2OC*n*)$_4$Cl (for *n* = 10, 14 and 18) and $Ru_2$(3,5-B2OC*n*)$_4$Cl (for *n* = 8, 10, 14 and 18)

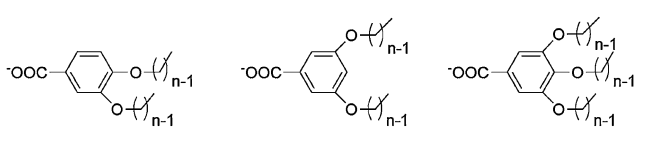


3,4-B2OC*n* 3,5-B2OC*n* 3,4,5-B4OC*n*

**Chart 2** Molecular schemes of the equatorial ligands used.

have been synthesized by methatesis reactions in which the equatorial butyrato ligands of the starting material $Ru_2[O_2C(CH_2)_2CH_3]_4Cl$[26] have been replaced by the corresponding alkoxybenzoato ligands. In a typical procedure, an ethanolic solution containing 0.2 mmol of $Ru_2[O_2C(CH_2)_2CH_3]_4Cl$ and *ca.* 2 mmol of the corresponding alkoxybenzoic acid was refluxed under Ar atmosphere up to total precipitation of a waxy red-brown product (the target compound and some free alkoxybenzoic acid). The desired compound was purified by dissolution in $CHCl_3$, addition of EtOH up to beginning of precipitation, then heating up to evaporation of $CHCl_3$, which aroused back to the total precipitation of the complex. This procedure was repeated until no-free acid was detected either by FTIR or by DSC. The product was dried under vacuum at 70 °C for 24 h. All the synthesized compounds were red-brown powders, except for the shorter homologues, that were waxy. Their characterization was carried out by IR spectroscopy as KBr pellets on either a Nicolet FTIR 510P or an Avatar FTIR 350 spectrometers, and by elemental analyses at *Servicio de Análisis a Terceros - Inquimae* (Carlo Erba CHNS-O EA1108). Microanalysis results and yield for each synthesis (Table S1†), IR features for each series of compounds (Table S2†) and details on some specific synthesis procedures are presented as ESI.† Some of the physicochemical studies described below (single-crystal crystallography, Exafs experiments, SQUID or Raman measurements) were used as additional evidence.

### Physicochemical measurements

Polarized-light optical microscopy observations (POM) as a function of temperature were carried out between cross polarizers on a Leitz DMRX microscope equipped with a Leitz 1350 hot-stage device. Transition temperatures and enthalpies were obtained by DSC experiments at a heating rate of 5 °C/min on a Shimadzu DSC-50.

The XRD patterns were obtained with two different experimental set-ups, the powder being filled in Lindemann capillaries of 1 mm diameter. A linear monochromatic Cu $K\alpha_1$ beam ($\lambda$ = 1.5418 Å) was obtained using a Guinier camera (900 W) or a Debye–Scherrer camera, both equipped with a bent quartz monochromator and an electric oven. A first set of diffraction patterns was registered with a gas curved counter "Inel CPS 120"; periodicities up to 60 Å can be measured, and the sample temperature is controlled within ±0.05 °C. The second set of diffraction patterns was registered on image plates; periodicities up to 90 Å can be measured, and the sample temperature is controlled within ±0.3 °C. Exposure times varied from 1 to 24 h. XRD patterns were recorded from room temperature to 200 °C.

Variable temperature IR experiments were conducted on an FTIR Nicolet 510P spectrometer using a home-made thermostatic chamber, equipped with CsCl windows, and heated with an electric resistance for experiments above room temperature or cooled with $N_2$(l) for experiments below room temperature. The temperature was monitored with a thermocouple inserted into the metallic block of the device. Resonance Raman experiments were performed at LASIR (CNRS, Paris) with a Dilor RTI triple monochromator spectrometer, using the 488 nm line of an Ar-laser. The powdered products were placed on a metallic sample holder, whose temperature was controlled with a home-made oven.

Dilatometry experiments were carried out on a Bekkedahl-type dilatometer. After placing a weighted amount of sample into a bulb of calibrated capillaries (0.5 to 1 g), vacuum was applied successively in the crystalline and the fluid phases, and then the system was immediately filled with freshly distilled mercury. Displaced volume of mercury was measured on a 0.01 mm scale during heating on a thermostatic bath (±0.01 °C). After the measurement, the capillary was evacuated, filled with Hg, and measured again.

The temperature dependence of the magnetic susceptibility was studied alternatively using a QD MPMS-XL susceptometer, or a QD-MPMS susceptometer, both operated at 5000 G between 2 and 400 K. The powdered samples, typically 10–50 mg, were placed in a small plastic pan (5 mm diameter). Raw magnetic data were corrected for the contribution from the sample holder and for the diamagnetism of the complexes. In order to evaluate this last contribution, the susceptibility of a similar but diamagnetic sample [$Rh_2$(3,5-B2OC18)$_4$] was also measured: the obtained value (mean molar $\chi$ in the whole temperature range = $-1.33 \times 10^{-3}$ emu), was certainly lower (approximately 50%) than the one calculated as a simple sum of Pascal's constants. We thus considered necessary, for such high molar mass compounds, to use this experimental value, corrected with Pascal's constants in order to account for both the different number of $CH_2$ units in the measured paramagnetic compound with respect to that of the diamagnetic reference, and the diamagnetism of the axial $Cl^-$ anion as well as that of Ru instead of Rh. Final used molar $\chi_{dia}$ values (emu): for $Ru_2$(3,5-B2OC18)$_4$Cl: $-1.38 \times 10^{-3}$; for $Ru_2$(3,4,5-B3OC10)$_4$Cl: $-1.14 \times 10^{-3}$; for $Ru_2$(3,4,5-B3OC14)$_4$Cl: $-1.71 \times 10^{-3}$.

Exafs experiments were conducted at the Exafs line of the Laboratorio Nacional de Luz Sincrotron (Campinhas, Brazil), working at 1.37 GeV with 150 mA (life-time: *ca.* 13 h), using the deflector magnet D04 (15°, $\sigma y$ = 0.222 mm), a Si(220) monochromator, and two ionization chamber detectors (before and after the sample) in the transmission mode. Samples were prepared as pressed pellets between either Maylar foils (room temperature experiments) or Kapton foils (high temperature experiments) in a stainless steel holder. A home-made oven (precision: ±1 °C) equipped with a thermocouple was used to thermostat the sample. Each experiment is the average of 3 to 5 spectra in the range 21900–23000 eV (K edge) taken over 3 s every 3 eV. A Mo foil (edge at 19999.5 eV) was used as calibrant, and Ru foils were used as reference. Data were processed with the software *EXAFS pour le MAC*;[27] $E^o$ was determined as the inflexion point; pseudo-radial distribution was filtered with a Kaiser window, and weighted by a $k^n$ factor (n = 2 for O or Cl and n = 3 for Ru retrodifuser atoms). $\lambda$ and $S_0$ parameters were obtained from measurements conducted on $Ru_2(O_2C_3H_7)_4Cl$ as reference, for which the crystalline structure is known,[28] thus $\Delta\sigma$ and $\Delta E^0$ (instead of $\sigma$ and $E^0$) were obtained from the fitting procedure.

Single crystals of $Ru_2$(3,4,5-B3OC2)$_4$Cl were obtained by slowly cooling a refluxed methanolic solution. Crystal Data were collected on a Bruker Smart CCD difractometer at 293 K using Mo $K\alpha$ radiation ($\lambda$ = 0.71073 Å). The structure was solved by direct methods and refined by full-matrix least squares on $F^2$,

using similarity restrainst between chemically equivalent bonds in order to circumvent a number of non-reasonable C–C bond distances appearing as a result of libration, *etc*. All non-hydrogen atoms were refined anisotropically; hydrogen atoms were idealized and allowed to ride both in coordinates as in displacement factors. Crystallographic data for $C_{52}H_{68}ClO_{20}Ru_2 \cdot 0.45(H_2O)$ (**1**): Mw = 1258.76, triclinic, space group $P\bar{1}$, a = 12.7209(17) Å, b = 14.6283(19) Å, c = 16.413(2) Å, Z = 2, $\alpha = 90.340(2)^\circ$, $\beta = 90.874(3)^\circ$, $\gamma = 100.198(2)^\circ$, V = 3005.5(7) Å$^3$, $D_c = 1.391$ g/cm$^3$, $\mu = 0.616$ mm$^{-1}$, F(000) = 1299, crystal size: 0.38 × 0.12 × 0.10 mm, from 15732 reflections collected 10326 were independent, of which 7834 had $I > 2\sigma(I)$ [$R_{int} = 0.069$]. The R values are R1 = 0.0647, and wR2 = 0.0907 [$I > 2\sigma(I)$] and GOOF = 1.058, max/min residual electron density: 1.26/−1.24 eÅ$^{-3}$. Programs used: data collection, SMART;[29] cell refinement, SAINT;[30] data reduction, SAINT; program(s) used to solve structure, SHELXS97;[31] program(s) used to refine structure, SHELXL97; molecular graphics, SHELXTL;[31] software used to prepare material for publication, SHELXTL.

## Results and discussion

### Phase sequence and mesomorphic properties: room temperature columnar mesogens

The phase sequences, transition temperatures, enthalpy changes and structural parameters were examined by POM, DSC and XRD. The main results are summarized in Table 1, and analyzed here for each series of compounds. Further structural information (detailed indexation for selected compounds at given temperatures) is presented in Table S3; representative DSC traces are shown in Fig. S1.†

**Table 1** Phase sequence and transition data of $Ru_2$(3,4,5-B3OC*n*)$_4$Cl, $Ru_2$(3,4-B2OC*n*)$_4$Cl, and $Ru_2$(3,5-B2OC*n*)$_4$Cl, compounds. The following abbreviations have been used for the phase nature: **Cr** (crystalline), **Col$_H$** (columnar hexagonal *p6mm* mesophase), **Col′$_H$** (a different **Col$_H$** mesophase), **Lam** (lamellar), **a.s.** (amorphous solid), or **I** (isotropic). Transition temperatures (in °C) and enthalpies (in kJ mol$^{-1}$, between parenthesis) are included between the corresponding phases. Also abbreviated: decomposition (dec), not determined (n.d.)

| Compound | Phase sequence |
|---|---|
| $Ru_2$(3,4,5-B3OC6)$_4$Cl | **Col$_H$** *c.a.* 300 (n.d.) **I**+ dec[a] |
| $Ru_2$(3,4,5-B3OC8)$_4$Cl | **Col$_H$** 294 (n.d.) **I** |
| $Ru_2$(3,4,5-B3OC10)$_4$Cl | **Cr** −35 (22) **Col$_H$** 290 (n.d.) **I** |
| $Ru_2$(3,4,5-B3OC12)$_4$Cl | **Cr** 0 (95) **Col$_H$** 297 (n.d.) **I** |
| $Ru_2$(3,4,5-B3OC14)$_4$Cl | **Cr** 25 (163) **Col$_H$** 285 (n.d.) **I** |
| $Ru_2$(3,4,5-B3OC16)$_4$Cl | **Cr** 41 (180) **Col$_H$** 284 (n.d.) **I** |
| $Ru_2$(3,4,5-B3OC18)$_4$Cl | **Cr** 58 (273) **Col$_H$** 266 (n.d.) **I** |
| $Ru_2$(3,4-B2OC10)$_4$Cl | **a.s.** *ca.* 100 (4) **Lam** 160 (4) **Col$_H$** 311 (n.d.) **I** + dec |
| $Ru_2$(3,4-B2OC14)$_4$Cl | **a.s.** *ca.* 80 (2) **Lam** 139 (3) **Col$_H$** 306 (n.d.) **I** + dec |
| $Ru_2$(3,4-B2OC18)$_4$Cl | **Cr** 26 (250) **a.s.** 74(3) **Lam** 129 (2) **Col$_H$** 290 (n.d.) **I** + dec |
| $Ru_2$(3,5-B2OC8)$_4$Cl | **Col′$_H$** 43 (4) **Col$_H$** 314 (n.d.) **I** + dec |
| $Ru_2$(3,5-B2OC10)$_4$Cl | **Col′$_H$** 58 (56) **Col$_H$** 312 (n.d.) **I** + dec |
| $Ru_2$(3,5-B2OC14)$_4$Cl | **Cr** −4 (60) **Col′$_H$** 60 (88) **Col$_H$** 302 (n.d.) **I** + dec |
| $Ru_2$(3,5-B2OC18)$_4$Cl | **Cr** 49 (150) **Col$_H$** 302 (n.d.) **I** + dec |

[a] No clear-cut transitions were detected either by POM or by DSC (from −90 °C to dec temperature).

**$Ru_2$(3,4,5-B3OC*n*)$_4$Cl series.** The shortest homologues (n = 6 to 12) of this series exhibit waxy room temperature phases, whose LC character was confirmed by XRD experiments. For the heaviest homologues, a transition from a crystalline phase to a LC mesophase was detected. The high viscosity of the mesophases prevented the development of unambiguous POM textures; however, in experiments conducted at very low heating rates, marbled textures compatible with columnar mesophases were observed. XRD experiments confirmed this assignment, and revealed their hexagonal nature (see below). Transition temperatures to the Col$_H$ mesophase increase monotonically with the chain length; for compounds with less than 14 carbon atoms per chain, the Col$_H$ mesophase is stable even below room temperature. The enthalpy of the Cr → Col$_H$ varies linearly with the aliphatic chain length (with the only exception of the n = 16 derivative, which shows deviating thermal and structural behavior in spite of its good chemical nature), following the equation ΔH (in kJ/mol) = 31.2 × *n* − 282.4. This linear relationship points towards a melting process dominated by the melting of the aliphatic chains (as usually accepted for columnar mesophases). The slope of this line corresponds to 2.6 kJ/mol per added methylene to the molecule, a value similar to the one found for other metallomesogenic bimetallic carboxylates,[20b, 32] and lower than the one found in smectics[33] or in simple paraphins.[34]

XRD patterns in the Col$_H$ mesophase showed a series of relatively sharp Bragg peaks in the reciprocal ratio 1:√3:√4:√7:√9:√12 (in some cases, even the √13 signal has been detected), corresponding to the 10, 11, 20, 21, 30, 22 (31) reflexions characteristic of a *p6mm* 2-D hexagonal order; Fig. 1 shows an example for $Ru_2$(3,4,5-B3OC12)$_4$Cl.

This hexagonal symmetry points towards a columnar hexagonal mesophase, well established after the number of reflexion peaks. The columnar surface S (calculated as the hexagonal section of a column, $S = \sqrt{3}/2\ a^2$, *a* being the parameter of the unit cell, $a = 2/\sqrt{3}\ d_{10}$) increases linearly with *n* (Fig. 2), following the equation: S (in Å$^2$) = 53 × *n* + 140 (parameters values stated for 90 °C). For all the compounds of this series, a thermal expansion of the hexagonal lattice has been observed, with thermal expansion coefficients [$\alpha(T) = \partial S/\partial T \times 1/S(T)$] of *ca.* 5 × 2 × 10$^{-4}$ K$^{-1}$. Also visible are diffuse Bragg peaks at *ca.* 6.1–6.5 Å, which does

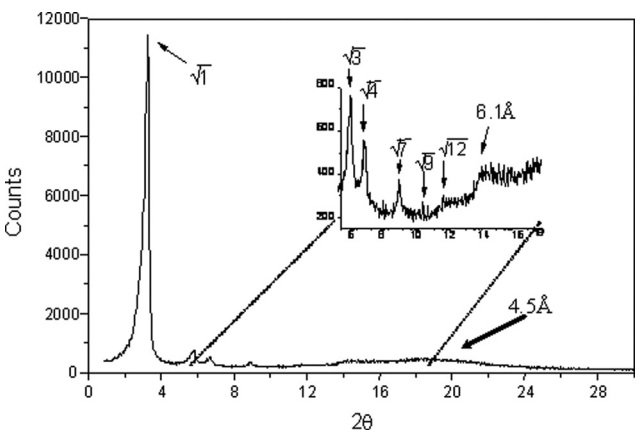


**Fig. 1** X-Ray diffraction pattern for $Ru_2$(B3OC12)$_4$Cl at 100 °C (Inel detector, exposure: 2 h).

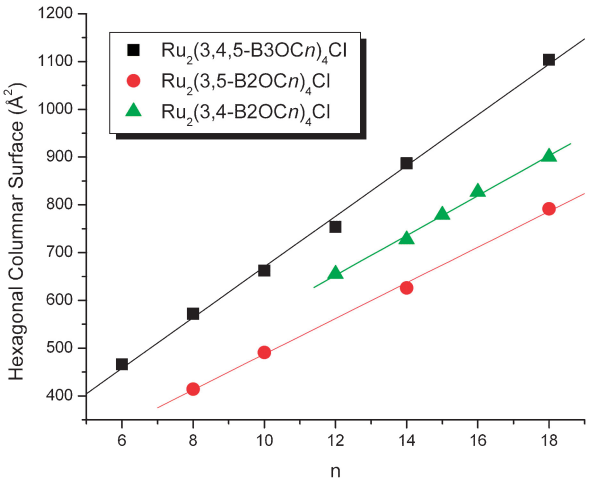


**Fig. 2** Hexagonal columnar surface as a function of the length of the aliphatic chains for the three $Ru_2(x,y,z\text{-B}m\text{OC}n)_4Cl$ series. Straight lines correspond to the fits described in the text, which do not include the points corresponding to $Ru_2(3,4\text{-B2OC10})_4Cl$ (transition temperature too close to the one used for the correlation) and $Ru_2(3,4,5\text{-B3OC16})_4Cl$ (see text). Plot includes both the results obtained in this work and results from previous studies.

not correspond to the hexagonal progression, but can be ascribed to the intracolumnar repeat distance (IRD), and at *ca.* 4.5 Å, ascribed to the molten methylenes.

**$Ru_2$(3,4-B2OC*n*)$_4$Cl series.** The presence of a high temperature columnar mesophase has been proposed in a preliminary work for some members of this series ($n$ = 12, 15, 16);[13b] the extension of these studies to the new synthesized $n$ = 10, 14 and 18 derivatives allows for comparisons along the whole series. At room temperature, all the studied derivatives are partly amorphous solids; they undergo a slow and wide transition to a different phase—characterized as lamellar owing to the 1:2:3 reciprocal spacing detected in the XRD patterns—at temperatures varying from 50 to 100 °C, depending on the chain length. At higher temperatures, they all exhibit a *p6mm* $Col_H$ mesophase that is not as well developed as in the case of the preceding series (only the 10, 11 and 20 reflections have been detected, in addition to the IRD at 5.7–5.8 Å and the 4.5 Å signal characteristic of molten aliphatic chains). Transition enthalpies to both the Lam and $Col_H$ mesophases are very low suggesting that the room temperature phase as well as the Lam phase is amorphous in nature, with a high degree of conformational disorder at the peripheral aliphatic chains. As in the preceding case, the columnar surface S increases linearly with chain length following, in this case the equation S (in Å$^2$) = 41.7 × $n$ + 153 (parameters values stated for 160 °C); the hexagonal lattice contracts with increasing temperature, with a thermal coefficient $\alpha = -1.1 \times 0.5 \times 10^{-3}$ K$^{-1}$.

**$Ru_2$(3,5-B2OC*n*)$_4$Cl series.** Melting to the mesophase takes place below room temperature for $n$ = 8, 10 and 14 derivatives, and approx. at 50 °C for the $n$ = 18 homologue. They exhibit marbled textures, compatible with columnar mesophases (as confirmed by XRD). In addition to the transitions collected in Table 1, a second endothermic peak was detected in DSC traces. This peak did not correlate with any change in texture or XRD patterns, and showed to be dependent on the thermal history of the compounds, disappearing after prolonged annealing; it is tentatively assigned to minor conformational changes of the aliphatic chains. Like the 3,4,5-series, compounds of the present 3,5-series exhibited very well developed XRD patterns corresponding to a *p6mm* hexagonal arrangement (10, 11, 20, 21, 22, 30 and 31 reflexions were easily detected as shown in Fig. S2†). On the basis of this progression, and the presence of a halo at 4.5 Å and a peak at 6.0 Å (IRD) on the diffraction patterns, this hexagonal mesophase can be identified as ordered $Col_H$. On the XRD patterns of all of the $Ru_2(3,5\text{-B2OC}n)_4Cl$ compounds it is also possible to see a small-angle Bragg peak corresponding to twice the $d_{10}$ (which was absent for the 3,4-series). A possible explanation for this "superstructure" is given in the ESI.† As in the preceding cases, the columnar surface S varies linearly with chain length, following in this case the equation S (in Å$^2$) = 37.4 × $n$ + 114 (parameters values stated for 100 °C). The hexagonal lattice expands when increasing temperature, with a thermal coefficient $\alpha = 1.0 \times 0.5 \times 10^{-3}$ K$^{-1}$.

All the studied compounds, with the exception of $Ru_2(3,4,5\text{-B3OC2})_4Cl$, exhibited columnar thermotropic mesophases. Fig. 3 shows the global thermal behavior of each of these three series, including both phase transitions temperatures and thermal decomposition temperatures. The series derived from the non-symmetric 3,4-B2OC*n* ligands is the only one to show mesomorphic polymorphism, the $Col_H$ phase being stabilized only above 140 °C; concomitantly, the XRD patterns for the 3,4-series show the less developed hexagonal order. This fact can tentatively be related to the number of molecular conformers compatible with these ligands (depicted in Chart S1†) however, in the absence of additional evidence, this suggestion cannot be further developed. On the other hand, the two series containing symmetric 3,5-B2OC*n* or 3,4,5-B3OC*n* ligands exhibit an easily accessible $Col_H$ mesophase; in fact, the thermal domain of the columnar mesophases of the 3,5- and 3,4,5- derivatives is remarkable, including cases where this $Col_H$ mesophase extends from well below 0 °C to *ca.* 300 °C.

## Local probes provide key insights to establish the molecular structure in the mesophase

A $Col_H$ mesophase with a high thermal stability including room temperature is a good starting point for ordered coordination polymers with potential applications. A good understanding of the intimate structure of the mesophase (a key factor for the physical properties) is necessary in order to advance further in this direction. The structural parameters determined by XRD look compatible with an hexagonal array of columns made up by single polymeric strand (which is not an obvious result: other related systems showed 2 or 4 strands/column).[13b,19] However, suggesting a model for the supramolecular organization of these compounds in the mesophase requires additional experimental information; the first step being the elucidation of the key features of the molecular structure in the mesophase. In order to do that, selected local probes, related to specific and characteristic aspects of the molecular structure have been used; the main results of these experiments are presented in this section.

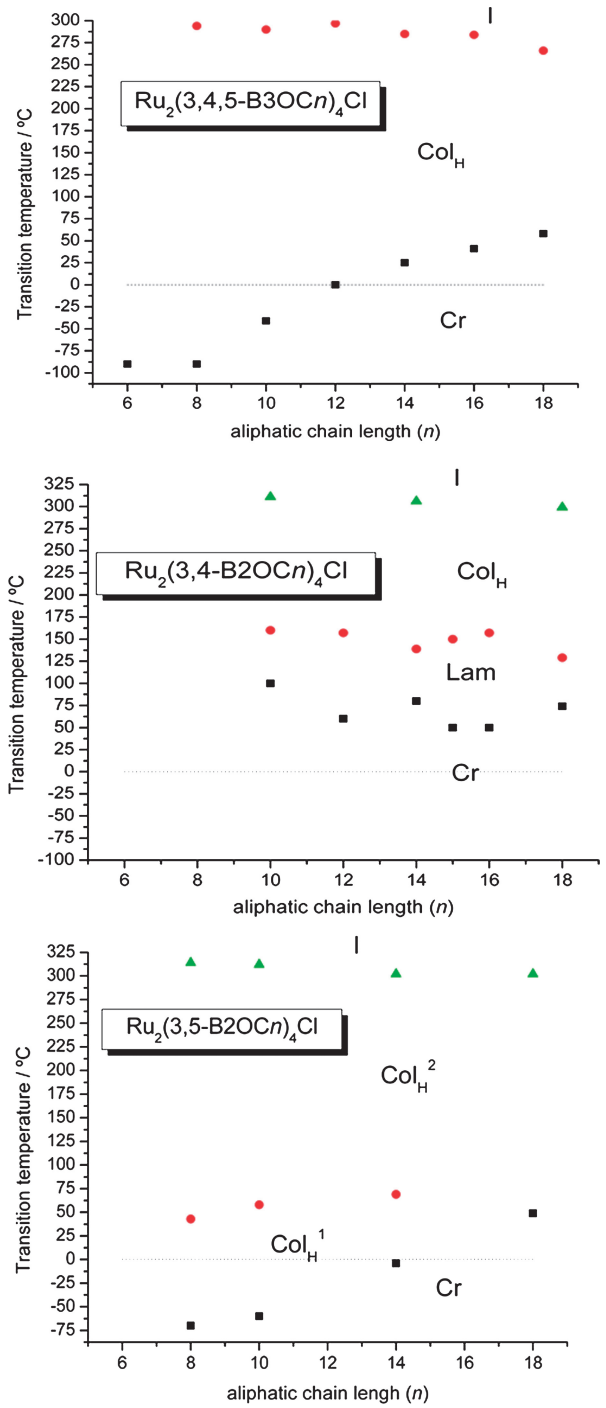


**Fig. 3** Transition temperatures and thermal domain stability for the different phases of the three studied series.

**Magnetic susceptibility.** Molecular magnetism is a very sensitive probe of the binuclear structure of these compounds. As it is well known, the presence of a S = 3/2 ground state undergoing a large zero field splitting is a direct result of the accidental degeneracy of the π* and δ* metal-metal MO, a distinctive signature of the diruthenium (II,III) systems with four carboxylates as equatorial ligands in a lantern structure.[21,35,36] We thus decided to perform variable temperature SQUID measurements for 3 compounds belonging to the two series exhibiting the $Col_H$

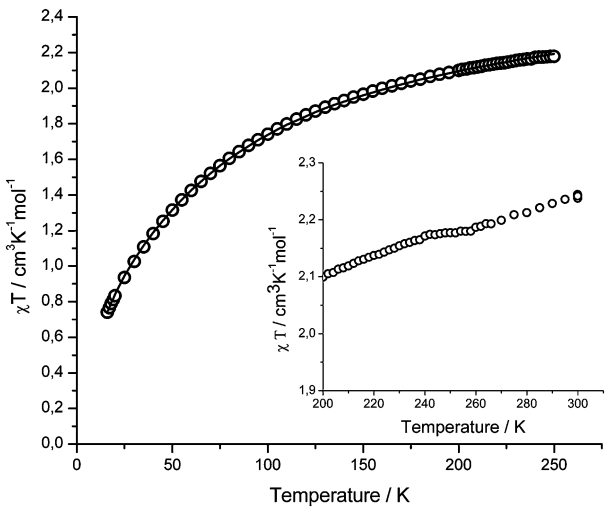


**Fig. 4** Magnetic behavior (χT as a function of temperature T) in the range 12–250 K for compound $Ru_2(3,4,5\text{-}B3OC10)_4Cl$; open circles are experimental data, the solid line correspond to the fit described in the text. The inset shows a detail of the product χ.T for the same compound at temperatures close to the Cr → $Col_H$ transition temperature (238 K after DSC).

mesophases at temperatures available to the SQUID systems; the three studied compounds were thus $Ru_2(3,5\text{-}B2OC18)_4Cl$, $Ru_2(3,4,5\text{-}B3OC10)_4Cl$ and $Ru_2(3,4,5\text{-}B3OC14)_4Cl$. The χT *vs.* T curve [shown in Fig. 4 for $Ru_2(3,4,5\text{-}B3OC10)_4Cl$ and in Fig. S3† for the two other compounds] is typical for mixed-valent diruthenium (II,III) tetracarboxylates; fitting of the experimental data with the usual models and equations (corresponding to slightly interacting S = 3/2 systems undergoing large ZFS)[14,22,35b,37] gave D = 80 $cm^{-1}$ and zJ = −0.3 $cm^{-1}$ for $Ru_2(3,5\text{-}B2OC18)_4Cl$, D = 77 $cm^{-1}$ and zJ = −2.3 $cm^{-1}$ for $Ru_2(3,4,5\text{-}B3OC10)_4Cl$, and D = 76 $cm^{-1}$ and zJ = −2,9 $cm^{-1}$ for $Ru_2(3,4,5\text{-}B3OC14)_4Cl$ (D is the zero-field splitting parameter corresponding to a H = S.D.S Hamiltonian and zJ is the interacting parameter in the framework of a molecular mean-field approximation). Please note that the use of a true Hamiltonian gives rise to the same energy levels than this effective Hamiltonian; very complete theoretical analysis of ZFS in mixed-valent diruthenium tetracarboxylates have been published recently.[36] Details on the fitting procedure as well as the complete set of parameters for each compound are given as supplementary material). As we are interested in the molecular changes that eventually take place at the transition to the mesophase, the χT *vs.* T curve at the transition temperature have been studied in detail: the inset in Fig. 4 shows that a very slight discontinuity is observed at the transition—similar results have been obtained for all the other compounds, a result that shows that the binuclear lantern structure (including the main features of the Ru–Ru bond) is essentially retained; only a very small diminution of χ can be noticed for both compounds, which might be ascribed to a small increase in the intermolecular antiferromagnetic interactions.

**Resonance Raman and IR spectroscopy.** In previous works on other mesogenic bimetallic carboxylates, variable-temperature IR spectroscopy showed small but detectable variations of some

specific vibration frequencies ($\nu CO_2$, $\nu CH_2$) when entering the mesophase.[38] We selected the $Ru_2$(3,4,5-B3OC14)$_4$Cl derivative in order to perform variable-temperature IR experiments, as its transition temperature (25 °C) allows for accessing both the crystalline and $Col_H$ phases with our experimental facilities. Successive IR spectra taken between −20 °C and 100 °C showed no detectable variation, a result that points in the same direction as the magnetic ones: the binuclear structure seems to remain essentially intact in the $Col_H$ phase.

A very characteristic feature of binuclear diruthenium tetracarboxylates is the Raman active $a_{1g}$ (in idealized $D_{4h}$ symmetry) Ru–Ru stretching at *ca.* 340 $cm^{-1}$, strongly enhanced by resonance.[11,35c, 39] We then performed variable temperature RR experiments on $Ru_2$(3,4,5-B3OC18)$_4$Cl, using λ = 488 nm for excitation in the π → π* transition. The spectra (the 20 °C spectrum corresponding to the crystalline phase is presented in Fig. 5) are dominated by the Ru–Ru stretching band (at 341 $cm^{-1}$ at 20 °C) and its first overtones (observed at 25 °C at 673, 1005 and 1309 $cm^{-1}$). Carboxylate stretchings (1586 and 1410 $cm^{-1}$ at 20 °C) and methylene deformations ($\delta^{\prime}CH_2$ at 1435 $cm^{-1}$ and $\nu CH_{2sym}$ at 1374 $cm^{-1}$ at 20 °C) can also be observed. Spectra taken at 45, 55, 65, 90 and 120 °C show that both $\nu Ru_2$ and its overtones slightly shift to lower frequencies in the mesophase (Table S5†). An analysis of the Morse parameters gave $\omega_e = 350$ $cm^{-1}$ and $\chi_e\omega_e = 4.2$ $cm^{-1}$ in the crystalline phase, and $\omega_e = 340 \pm 1$ $cm^{-1}$ and $\chi_e\omega_e = 2.1 \pm 0.4$ $cm^{-1}$ in the mesophase (see inset of Fig. 5, the slight difference with the transition temperature detected by DSC is ascribed to local heating).[35c] There is a concomitant shift (−4 $cm^{-1}$) in the symmetric $CO_2$ stretching, whereas vibrations corresponding to both phenyl rings and aliphatic chains methylenes remain constant. These variations point to a very slight softening of the Ru–Ru bond, possibly accompanied by a slight strengthening of the axial Ru–Cl bond, in agreement with magnetic results.

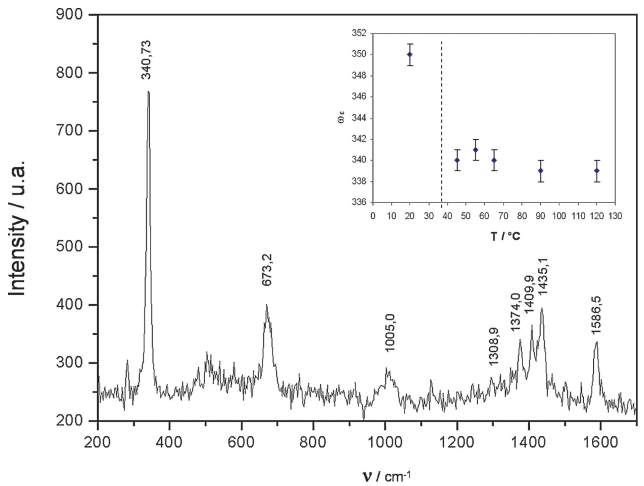


**Fig. 5** A resonance Raman spectrum of $Ru_2$(3,4,5-B3OC18)$_4$Cl at 20 °C ($\lambda_{exc}$ = 488 nm, laser power 0.015 mW). ν(RuRu) and its first three overtones are visible, as well as other vibrations corresponding to the equatorial ligands (see Table S5† for assignments). The inset shows the temperature dependence of the equilibrium frequency ($\omega_e$) corresponding to the Morse potential of Ru–Ru stretching, (the dashed line shows the Cr → $Col_H$ transition temperature).

**Exafs.** $Ru_2$(3,4,5-B3OC10)$_4$Cl was selected for Exafs experiments as its $Col_H$ mesophase is available even at room temperature. Two spectra have been recorded, at 25 °C and at 100 °C, and corrected as explained in the experimental section. The obtained pseudo-radial distribution for the compound at 25 °C (Fig. 6) shows two different shells, which could not be completely resolved. The first one, centered at 1.4 Å, corresponds to the coordinating O atoms; the second one, approximately at 1.9 Å, corresponds to the second Ru atom from each dimer, and likely includes the axial $Cl^-$ contribution to retrodiffusion.[40]

Refinement of the FT of the first shell, taken from 1.14 to 1.47Å, gave N = 4.08 oxygen atoms at a mean distance R = 1.99 Å; the second shell (taken from 1.58 to 2.17 Å) gave N = 0.93 Ru atoms at R = 2.30 Å. Fig. 6 (insets) shows the excellent agreement between the experimental and calculated $\chi k^n$ values for

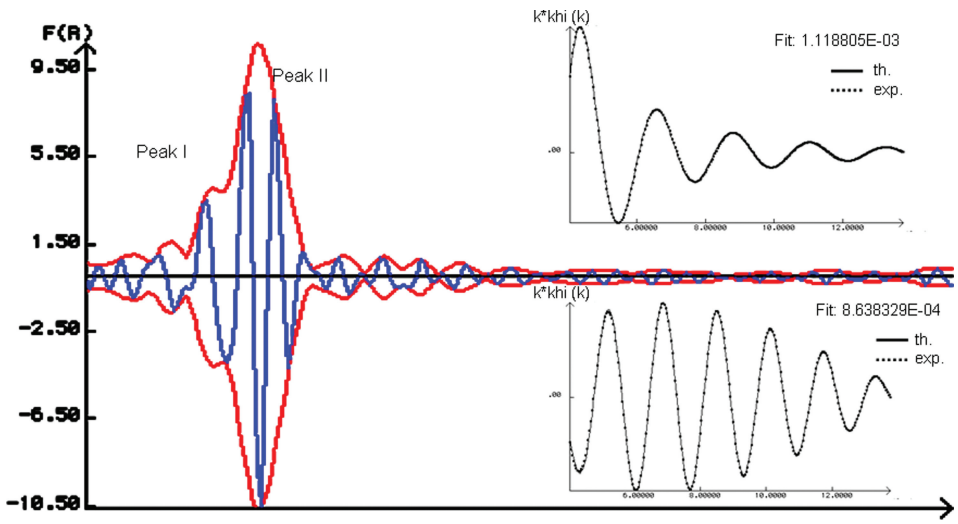


**Fig. 6** Pseudo-radial distribution from the 25 °C Exafs spectrum of $Ru_2$(3,4,5,-B3OC10)$_4$Cl and refinement of the first peak (upper inset) and second peak (lower inset) as described in the text.

both shells, detailed final parameters are presented in Table S6.† The second spectrum, obtained at 100 °C, shows a TF similar to the one obtained at 25 °C, satisfactorily fitted with N = 4.04 O atoms at R = 1.99 Å and N = 0.84 Ru atoms at R = 2.29 Å (see Table S6† for the whole set of parameters).

**A structural model for the supramolecular organization in the mesophase.** Local probes have clearly shown that the binuclear molecular structure characteristic of the crystalline phase of diruthenium tetracarboxylates is kept in the mesophase, and should be considered as the building block of the supramolecular architecture of the $Col_H$ mesophase. The linear progression of the columnar surface as a function of the aliphatic chain length for each of the three studied series (see Fig. 2) agrees well with the accepted model for columnar mesophases: interacting cores surrounded by conformationally disordered (liquid-like) aliphatic chains.[41,42] The interaction between cores is primarily due in the present case to the coordination Ru–Cl bond, thus the main parameter to be considered for any structural model is the intracolumnar repeat distance, *h*. As stated above, we evaluated this intracolumnar repeat distance from the peak in XRD patterns as 6.3, 5.8 and 6.0 Å for $Ru_2$(3,4,5-B3OC*n*)$_4$Cl, $Ru_2$(3,4-B2OC*n*)$_4$Cl and $Ru_2$(3,5-B2OC*n*)$_4$Cl respectively.

*h* values can also be estimated by two other independent ways. In the first one, we followed an usual approach in the structural analysis of columnar mesophases,[13b, 25,42,43] considering that the volume of one columnar repeat unit, centered on one node of the hexagonal array, with the transversal section area S and height *h*, can be expressed as

$$V = Sh = pV_o \quad (1)$$

where $V_o$ is the volume of one binuclear unit and p the number of binuclear units within the columnar section. If molar volumes are assumed to be additive, the volume $V_o$ can be written as

$$V_o = V_{pc} + 4m(nVCH_2 + \Delta VCH_3) \quad (2)$$

where *n* is the number of carbon atoms in each alkyl chain, *m* is the number of alkoxy chains on each aromatic ring; $V_{pc}$ is the molecular volume of the polar core; $VCH_2$ and $\Delta VCH_3$ are the molecular volumes of the methylene group and the difference between methyl and methylene groups respectively. By replacing $V_o$ in eqn 1 with the latter expression, the cross-section area of a column becomes:

$$S = (p/h)[V_{pc} + 4m\Delta VCH_3] + (p/h)[4mVCH_2]n \quad (3)$$

The first term, independent of *n*, is a constant for each series; the second term increases linearly with *n*, with slope (p/*h*)[4*m*$VCH_2$], whose value depends on the p, *h* and *m* parameters characteristic of each series. The value of p/*h* was thus calculated from the slope obtained by linear regression of the experimental S *vs*. *n* data. The values of $VCH_2$(T) and $\Delta VCH_3$(T), for aliphatic chains in a disordered conformation, were taken from the literature[44] as $VCH_2(T) = 26.5616 + 0.02023T$ (Å$^3$/methylene), and $\Delta VCH_3(T) = 27.14 + 0.01713T + 0.0004181T^2$ (Å$^3$/methylene), where the temperature T is in °C. This procedure lead to h/*p* values of 6.2 (0.2), 5.7 (0.2) and 6.0 (0.2) Å[45] for $Ru_2$(3,4,5-B3OC*n*)$_4$Cl, $Ru_2$(3,4-B2OC*n*)$_4$Cl and $Ru_2$(3,5-B2OC*n*)$_4$Cl respectively, which are in excellent agreement with the values obtained from XRD experiments (IRD peak).

In order to validate the assumption that the molar volumes are additive, we compared the mean molecular volume ($V_o$) derived from the XRD data ($V_o = Sh$, as p = 1) with the molecular volumes estimated ($V_e$) by adding the volumes of the different molecular parts (see ESI† for details on these calculations and detailed comparison results). All the experimental values $V_o$ agree with the calculated $V_e$ values within the experimental uncertainty (5–7%). Additional support for this calculation came from an experimental determination of the molecular volume of one compound [$Ru_2$(3,4,5-B3OC10)$_4$Cl] by dilatometry (see Fig. S4†): the temperature dependence of its molecular volume follow the equation V (in Å$^3$) = 4036.3 + 2.949T (T in °C), giving a value of 4302 Å$^3$ at 90 °C, in very good agreement with the estimated $V_e$ = 4143 Å$^3$.

It is necessary to point out that these intracolumnar repeat distances are short compared to the expected interdimeric distance calculated on the basis of the known crystallographic Ru–Ru and Ru–Cl distances; indeed, the expected repeat distance, calculated as 2 $d_{Ru-Cl}$ + $d_{Ru-Ru}$, sum up 7.41 (0.05) Å. However, this estimation holds for a completely extended polymeric strand, with Ru–Cl–Ru and Ru–Ru–Cl angles of 180°. The difference between this 7.41 Å value and the calculated *h* values can be explained if the polar cores are tilted with respect to the columnar axis (Fig. 7). Following simple planar geometrical considerations, the interdimer ($Ru_2$)–Cl–($Ru_2$) (φ) angle can be estimated from the previous *h* values as 112(5)°, 101(6)° and 108(6)° for the $Ru_2$(3,4,5-B3OC*n*)$_4$Cl, $Ru_2$(3,4-B2OC*n*)$_4$Cl and $Ru_2$(3,5-B2OC*n*)$_4$Cl series respectively. Such zig-zag conformations are often found in polymeric $Ru_2(O_2CR)_4Cl$ compounds, for which Ru–Cl–Ru angles ranging from 110 to 142° (apart the linear 180° conformations) have been observed.[11,14d] The calculated angles based on the *h* distance seem quite low when compared to these values; however, it should be taken into account that φ includes both the Ru–Cl–Ru and Ru–Ru–Cl angles; moreover, a detailed analysis of the published crystallographic structures shows that Ru–Ru, Ru–Cl, Cl–Ru and the next Ru–Ru bonds are not coplanar, but zig-zag in both directions (Fig. 8), reducing further the repetition distance. In fact,

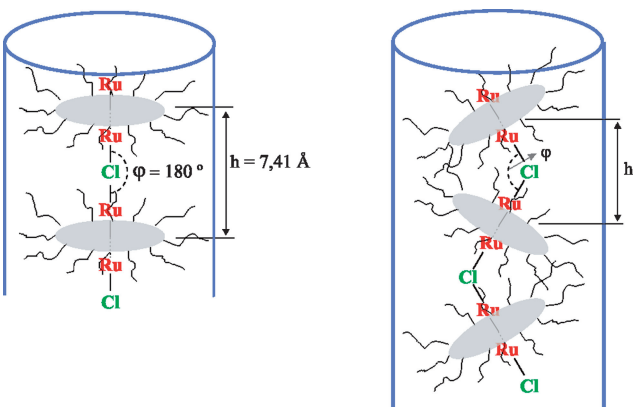


**Fig. 7** A schematic depiction of the suggested model for the structure of the $Col_H$ mesophases of the studied compounds.

this distance, calculated from published crystallographic data for the compounds exhibiting Ru–Cl–Ru angles shorter than 120°, lies in the 6.0–6.6 Å range.

It should be pointed out that the true repetition distance in the model depicted in Fig. 7 is twice the interdimer *h* distance, chlorine, carbon and oxygen atoms being not in the same positions in neighboring binuclear units. However, owing to the fact that X-rays mainly interact with the heavy atoms, and that both Ru atoms are very close in distance, the ensemble $Ru_2$ will act as a single diffraction element, giving rise to diffraction peaks corresponding to *h*, instead of the 2*h* resulting from the non-equivalent neighboring $Ru_2$ orientations.

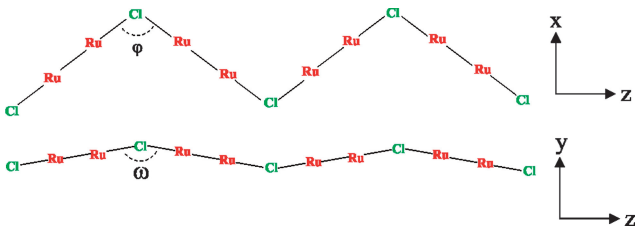


**Fig. 8** Conformational details of the $Ru_2$–Cl–$Ru_2$–Cl– strands from published crystallographic studies.

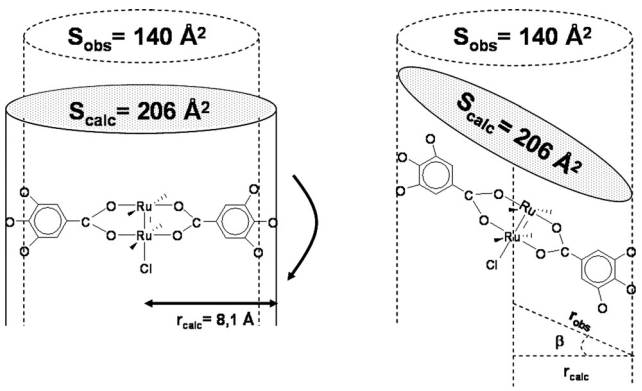


**Fig. 9** Tilting of the polar cores produces a projected surface compatible with the one calculated from the intercept of the S *vs.* *n* plots.

A third independent way to calculate *h* values, providing additional evidence for the suggested model, is based on the analysis of the intercept of the S *vs.* T plots. The physical meaning of this intercept is the surface of the molecular parts independent from *n*, *i.e.* the polar core contribution, and the terminal methyl group contribution. The radius of the polar core, calculated from crystallographic studies as the distance from the central Ru atom to the oxygen atoms attached to the phenyl group,[46] can be estimated as 8.1(0.2) Å for all the three series; the circle containing the polar core having thus a surface of *ca.* 206(5) Å$^2$. This surface is wider that those calculated from the intercepts of the S *vs.* *n* plots, but can be compatible if the core is assumed to be tilted with respect to the columnar axis (Fig. 9), as in the previous analysis based on the slope of this plot, and on experimental XRD data. The tilting angles (β) calculated by comparison of these surfaces are 34, 42 and 30°, in good agreement with the previously calculated φ angles (β should be half the supplement of φ in this model), taking into account the comments summarized in Fig. 8.

## The crystalline structure of a light homologue supports the structural model for the mesophase

The final proof for the plausibility of this model arises from the crystalline structure of one homologue of these series (CIF file included as ESI†). As no structure had been published up to date for this kind of compounds [diruthenium di- or tri-(alkoxy)benzoates], we undertook the synthesis of a short-chain homologue of the trisubstituted series [namely, $Ru_2$(3,4,5-B3OC2)$_4$Cl], as well as its crystal structure resolution. $Ru_2$(3,4,5-B3OC2)$_4$Cl crystallizes from methanol in the P$\bar{1}$ group. Its molecular structure corresponds to the typical lantern structure, built up around a crystallographic symmetry center. Each Ru atom is in a slightly distorted octahedral environment (Fig. S6†), with Ru–Ru, Ru–O and Ru–Cl distances (Table S8†) typical for diruthenium tetracarboxylates.[11] The phenyl rings of the

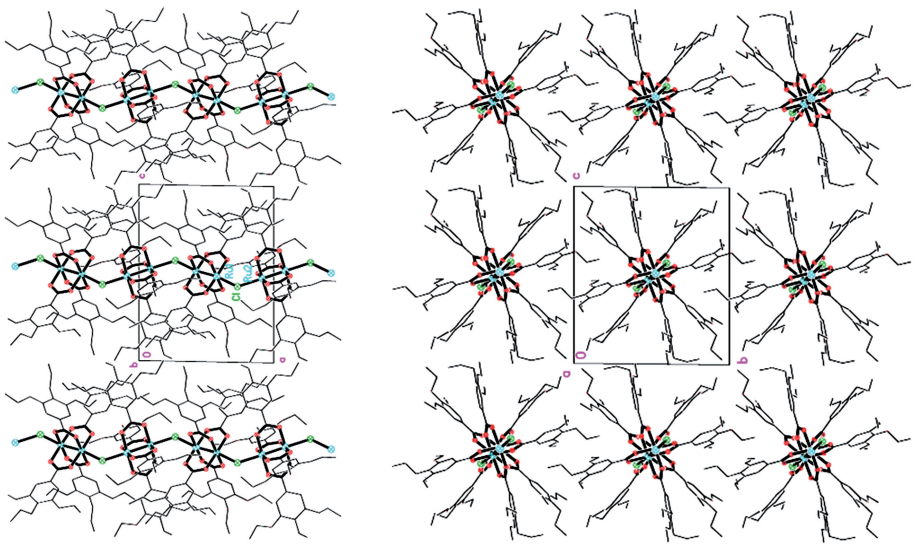

**Fig. 10** Packing along the b and c axis for $Ru_2$(3,4,5-B3OC2)$_4$Cl.

equatorial carboxylates are tilted by 10.2, 2.7 and 13.4° (moieties A, B and C) with respect to the planes of the carboxylate groups. Each chloride anion is coordinated to the axial positions of two different bimetallic units, giving rise to a polymeric structure, which extends along the *a* axis. As suggested in our model for the supramolecular architecture of the heavier homologues in the columnar mesophase, these polymeric strands adopt a *zig-zag* conformation, whose origin likely includes orbital overlap and packing constraints.[35d] Moreover, the experimental Ru–Cl–Ru = 117° and Ru–Ru–Cl = 170 and 172° angles agree well with the predicted values, and give rise to a repetition distance (Ru1–Ru2′ associated to O1C) of 6.44–6.48 Å, very close to the $h = 6.1$–6.4 Å values found by 3 independent ways for $Ru_2(3,4,5\text{-}B3OCn)_4Cl$ compounds in our structural analysis. Our previous estimation of the polar core radius (8.1 Å) is fully confirmed in this crystalline structure, where a value of 8.2 Å is found. Finally, the structure shows (Fig. 10), as predicted, the required organization of the polymeric strands: they run parallel to each other, confirming that the use of these bulky carboxylates efficiently fill the inter-dimeric space, thus avoiding perpendicular arrangements like the ones found for $Ru_2(O_2C_4H_3)_4Cl$ and $Ru_2(O_2C_5H_9)_4Cl$. The present crystalline structure shows the required arrangement of the polymeric strands, preconfiguring the columnar structure.

## Conclusions

The use of di- or tri-alkoxybenzoates as equatorial ligands, a strategy already used in "neutral" $Rh_2$(II,II) polymeric materials in order to fill the intermolecular space in an intracolumnar way,[25] was also successful for the present "ionic" coordination polymers based in the interesting $Ru_2$(II,III) unit. Indeed, we obtained compounds for which the columnar mesophase appears even well below room temperature, and extends in some cases to *ca*. 300 °C. The key positions at which the long chains should be attached to the phenyl rings are the 3,5-(*meta*-)positions: thermal properties of the 3,5- and 3,4,5- substituted benzoates are very similar, and certainly more interesting (room temperature mesophases) than those of the 3,4- substituted derivatives. This synthesis strategy can be extended to the molecular design of columnar LC order in other spinal coordination polymers where, in spite of very good electronic communication along the polymeric backbone, the LC character remained elusive.

The combined use of macrostructural information and local spectroscopic or magnetic probes allowed us to suggest a detailed model of the supramolecular architecture of the three studied series, including structural parameter values, further validated by crystallographic studies. The global picture is that of hexagonal array of columns, each column including a central $\cdots Ru_2(O_2C)_4$–Cl–$\cdots$ strand in *zig-zag* conformation, surrounded by molten aliphatic chains. This model supports the usual description of columnar mesophases (a compromise between "ordering" interactions among the flat central cores of the discoid mesogens and the "disordering" tendency of the conformationally disordered aliphatic chains). It also provides a structural basis for further analysis of the physical properties of these materials. An appropriate connection between the bimetallic centers in these 1-D systems, could give rise to interesting materials with proved high thermal stability and potential transport properties along the columns, which might be macroscopically oriented from their lyotropic mesophases. Such explorations are currently under way in our labs.

## Acknowledgements

We thank the very kind people who helped us in different physicochemical studies: Dr Olivier Poizat and Gérard Sagon (LASIR) for Resonance Raman experiments, Richard Poinsot (IPCMS), Jean-Francois Jacquot and Dr Roberto Calemczuk (CEA) for SQUID measurements, Dr A. Michalowicz for providing us with the software for EXAFS data analysis and Rosana Gomez and María de los Angeles Persello (UNGS) for carefully growing the single-crystals. We are indebted to Dr Maria do Carmen Martin Alves (LNLS) for her kind assistance in EXAFS measurements; the Laboratorio Nacional de Lus Sincrotron (LNLS-Campinhas-Brazil) is also acknowledged. We acknowledge the Spanish Research Council (CSIC) for providing us with a free-of-charge license for the CSD system. Grants from the University of Buenos Aires (AX27, X219), Conicet (PEI 221/97, PIP 02568), ANPCyT (PICT 06-25409) and Setcip-Ecos (International Cooperation A01E05), as well as fellowships from Conicet to MR, MAC and ZC supported this work. FDC is a member of the research staff of Conicet.

## References

1 S. Kitagawa and S. Noro, in *Compr. Coord. Chem.*, ed. J. Mc Cleverty and T. J. Meyer, Elsevier Pergamon, Amsterdam, 2004, vol. 7, pp. 231–262.
2 E. C. Constable, in *Compr. Coord. Chem.*, ed. J. Mc Cleverty and T. J. Meyer, Elsevier Pergamon, Amsterdam, 2004, vol. 7, pp. 263–302.
3 C. T. Chen and K. S. Suslick, *Coord. Chem. Rev.*, 1993, **128**, 293–322.
4 J. Simon, J. J. André and A. Skoulios, *New J. Chem.*, 1986, **10**, 295–311.
5 H. Iwamura and K. Inoue, in *Magnetism: Molecules to Materials II*, ed. J. S. Miller and M. Drillon, Wiley-VCH, Wheinheim, 2001, 61–108; O. Kahn, *Acc. Chem. Res.*, 2000, **33**, 647–657.
6 G. E. Kellog and J. G. Gaudiello, in *Inorganic Materials*, ed. D. Bruce and D. O'Hare, John Wiley & Sons, Chichester, 2nd edn, 1996, pp. 378–428.
7 M. Hanack and M. Lang, *Adv. Mater.*, 1994, **6**, 819–833.
8 N. B. McKeown, *J. Mater. Chem.*, 2000, **10**, 1979–1995.
9 M. Pilkington and S. Decurtins, in *Magnetism: Molecules to Materials II*, ed. J. S. Miller and M. Drillon, Wiley-VCH, Wheinheim, 2001, pp. 339–356.
10 (*a*) O. Sato, T. Iyoda, A. Fujishima and K. Hashimoto, *Science*, 1996, **271**, 49; (*b*) M. Verdaguer, *Science*, 1996, **272**, 698; (*c*) K. R. Dumbar and R. A. Heintz, *Prog. Inorg. Chem.*, 1997, **45**, 283.
11 (*a*) M. A. S. Aquino, *Coord. Chem. Rev.*, 1998, **170**, 141–202; (*b*) M. A. S. Aquino, *Coord. Chem. Rev.*, 2004, **248**, 1025–1045.
12 P. Angaridis, in *Multiple Bonds Between Metal Atoms*, ed. F. A. Cotton, C. A. Murillo and R. A. Walton, Springer Science and Bussines Media Inc., New York, 3rd edn, 2005.
13 (*a*) F. D. Cukiernik, M. Ibn-Elhaj, P. Maldivi, A. M. Giroud-Godquin, D. Guillon, J. C. Marchon and A. Skoulios, *Liq. Cryst.*, 1991, **9**, 903–908; (*b*) F. D. Cukiernik, M. Ibn-Elhaj, Z. Chaia, J. C. Marchon, A. M. Giroud, D. Guillon, A. Skoulios and P. Maldivi, *Chem. Mater.*, 1998, **10**, 83–91; (*c*) J. F. Caplan, C. A. Murphy, S. Swansburg, R. P. Lemieux, T. S. Cameron and M. A. S. Aquino, *Can. J. Chem.*, 1998, **76**, 1520–1523.
14 (*a*) T. E. Vos, Y. Liao, W. W. Shum, J.-H. Her, P. W. Stephens, W. M. Reiff and J. S. Miller, *J. Am. Chem. Soc.*, 2004, **126**, 11630–11639; (*b*) T. E. Vos and J. S. Miller, *Angew. Chem., Int. Ed.*, 2005, **44**, 2416–2419; (*c*) D. Yoshioka, M. Mikuriya and M. Handa, *Chem. Lett.*, 2002, 1044–1045; (*d*) M. Mikuriya, D. Yoshioka and M. Handa, *Coord. Chem. Rev.*, 2006, **250**, 2194–2211.
15 A. M. Giroud-Godquin, *Coord. Chem. Rev.*, 1998, **178–180**, 1485–1499.

 

16 B. Donnio, D. Guillon, R. Deschenaux, D. W. Bruce in *Compr. Coord. Chem.*, ed. J. Mc Cleverty and T. J. Meyer, Elsevier Pergamon, Amsterdam, 2004, vol. 7, pp. 359–627.
17 *Metallomesogens*, ed. J. L. Serrano, VCH Weinheim, 1996.
18 (*a*) D. W. Bruce, in *Inorganic Materials*, ed. D. W. Bruce and D. O'Hare, John Wiley & Sons, Chichester, 2nd edn, 1996, pp. 422–522; (*b*) P. Espinet, M. A. Esteruelas, L. A. Oro, J. L. Serrano and E. Sola, *Coord. Chem. Rev.*, 1992, **117**, 215–274; (*c*) A. M. Giroud-Godquin and P. M. Maitlis, *Angew. Chem. Int., Ed. Engl.*, 1991, **30**, 375–402; (*d*) A. M. Giroud-Godquin, in *Handbook of Liquid Crystals*, ed. D. Demus, J. Goodby, G. W. Gray, H. W. Spiess and V. Vill, Wiley-VCH, Weinheim, 1998, vol. 2B, pp. 901–932; (*e*) B. Donnio and D. Bruce, *Str. Bonding*, 1999, **95**, 193–247; (*f*) F. Neve, *Adv. Mater.*, 1996, **8**, 277–289; (*g*) L. Oriol and J. L. Serrano, *Adv. Mater.*, 1995, **7**, 348–369.
19 Z. Chaia, A. Zelcer, B. Donnio, M. Rusjan, F. D. Cukiernik and D. Guillon, *Liq. Cryst.*, 2004, **31**, 1019–1025.
20 (*a*) J. C. Marchon, P. Maldivi, A. M. Giroud-Godquin, D. Guillon, M. Ibn-Elhaj and A. Skoulios, in *Nanostructures based on Molecular Materials*, ed. W. Gopel and C. Ziegler, VCH, Weinheim, 1992, pp. 285; (*b*) P. Maldivi, PhD Thesis, Université Grenoble I, 1989; (*c*) M. Ibn-Elhaj, D. Guillon, A. Skoulios, A. M. Giroud-Godquin and P. Maldivi, *P. Liq. Cryst.*, 1992, **11**, 731–744.
21 M. J. Bennet, K. G. Caulton and F. A. Cotton, *Inorg. Chem.*, 1969, **8**, 1–6.
22 F. D. Cukiernik, D. Luneau, J. C. Marchon and P. Maldivi, *Inorg. Chem.*, 1998, **37**, 3698–3704.
23 (*a*) M. Rusjan, E. E. Sileo and F. D. Cukiernik, *Solid State Ionics*, 1999, **124**, 143–147; (*b*) M. Rusjan, E. E. Sileo and F. D. Cukiernik, *Solid State Ionics*, 2003, **159**, 389–396.
24 Z. D. Chaia, B. Heinrich, F. D. Cukiernik and D. Guillon, *Mol. Cryst. Liq. Cryst.*, 1999, **330**, 213–220.
25 M. Rusjan, B. Donnio, D. Guillon and F. D. Cukiernik, *Chem. Mater.*, 2002, **14**, 1564–1575; J. Barberá, M. A. Esteruelas, A. M. Levelut, L. A. Oro, J. L. Serrano and E. Sola, *Inorg. Chem.*, 1992, **31**, 732–737 (compare with compound 9).
26 E. Forest, P. Maldivi, J. C. Marchon and H. Virelizier, *Spectroscopy*, 1987, **5**, 129.
27 A. Michalowicz, in *Logiciel pour la Chimie*, Societe Francaise de Chimie Ed., Paris, 1991, pp. 102.
28 A. Bino, F. A. Cotton and T. Felthouse, *Inorg. Chem.*, 1979, **18**, 2599–2604.
29 Bruker 2001. *SMART-NT V5.624. Data Collection Software*, Siemens Analytical X-ray Instruments Inc., Madison, Wisconsin, USA.
30 Bruker 2002. *SAINT-NT V6.22a (Including SADABS). Data Reduction Software*, Siemens Analytical X-ray Instruments Inc., Madison, Wisconsin, USA.
31 G. M. Sheldrick, *Acta Cryst. A*, 2008, **64**, 112–122.
32 H. Abied, D. Guillon, A. Skoulios, P. Weber, A. M. Giroud-Godquin and J. C. Marchon, *Liq. Cryst.*, 1987, **2**, 269–279.
33 P. Seurin, D. Guillon and A. Skoulios, *Mol. Cryst. Liq. Cryst.*, 1981, **65**, 85–110.
34 *Handbook of Chemistry and Physics*, ed. R. C. Weast, 66th edn 1986, CRC Press.
35 (*a*) J. G. Norman, G. E. Renzoni and D. Case, *J. Am. Chem. Soc.*, 1979, **101**, 5256–5267; (*b*) J. Telser and R. S. Drago, *Inorg. Chem.*, 1984, **23**, 3114–3120; corrected in J. Telser, V. M. Miskowski, R. S. Drago and N. M. Wong, *Inorg. Chem.*, 1985, **24**, 4765; (*c*) G. Estiú, F. D. Cukiernik, O. Poizat and P. Maldivi, *Inorg. Chem.*, 1999, **38**, 3030–3039; (*d*) M. A. Castro, A. E. Roitberg and F. D. Cukiernik, *Inorg. Chem.*, 2008, **47**, 4682–4690.
36 W. W. Shum, Y. Liao and J. S. Miller, *J. Phys. Chem. A*, 2004, **108**, 7460–7462.
37 (*a*) F. D. Cukiernik, A. M. Giroud-Godquin, P. Maldivi and J. C. Marchon, *Inorg. Chim. Acta*, 1994, **215**, 203–208; (*b*) E. J. Beck, K. D. Drysdale, L. K. Thompson, L. Li, C. A. Murphy and M. A. S. Aquino, *Inorg. Chim. Acta*, 1998, **279**, 121–125; (*c*) M. Handa, D. Yoshioka, Y. Suyama, K. Shiomi, M. Mikuriya, I. Hiromitsu and K. Kasuga, *Chem. Lett.*, 1999, 1033–1034; (*d*) M. C. Barral, R. Jimenez-Aparicio, D. Perez-Quintanilla, J. L. Priego, E. C. Royer, M. R. Torres and F. A. Urbanos, *Inorg. Chem.*, 2000, **39**, 65–70.
38 D. P. Strommenn, A. M. Giroud-Godquin, P. Maldivi and J. C. Marchon, *Liq. Cryst.*, 1987, **2**, 689–699.
39 (*a*) R. J. H. Clark and L. T. H. Ferris, *Inorg. Chem.*, 1981, **20**, 2579–2585; (*b*) V. M. Miskowski, T. M. Loher and H. B. Gray, *Inorg. Chem.*, 1987, **26**, 1098–1107.
40 A proper treatement of the spectra requires the inclusion of Cl as a retrodifusive atom; however, its inclusion rises excessively the number of parameters to be fitted, precluding confident results. Omission of Cl is an acceptable choice owing to the big difference in electrons number with respect to Ru, confirmed by the insensitivity of the fits to its inclusion.
41 (*a*) S. Chandrasekhar, in *Handbook of Liquid Crystals*, ed. D. Demus, J. Goodby, G. W. Gray, H. W. Spiess and V. Vill, Wiley-VCH, Weinheim, 1998, vol. 2B, pp. 749–779; (*b*) D. M. Collard and P. Lillya, *J. Am. Chem. Soc.*, 1991, **113**, 8577–8583.
42 D. Guillon, *Struct. Bonding (Berlin)*, 1999, **95**, 42–82.
43 A. M. Levelut, *J. Chim. Phys.*, 1983, **80**, 149–161.
44 D. Guillon, A. Skoulios and J. J. Benattar, *J. Phys.*, 1986, **47**, 133.
45 Uncertainty includes both refinement uncertainties and differences among the various homologues of each series.
46 B. K. Das and A. R. Chakravarty, *Polyhedron*, 1991, **10**, 491–494.